Applied Problems of Nonlinear Oscillation and Wave Theory

Izvestiya Vysshikh Uchebnykh Zavedeniy. Applied Nonlinear Dynamics. 2025;33(4)

Article DOI: 10.18500/0869-6632-003167

Dynamic model of economic cycles origin

V. V. Matrosov✉, *V. D. Shalfeev*

National Research Lobachevsky State University of Nizhny Novgorod, Russia
E-mail: ✉matrosov@rf.unn.ru, shalfeev@rf.unn.ru

Received 10.12.2024, accepted 22.02.2025, available online 7.03.2025, published 31.07.2025

Abstract. *Purpose* of the work is to research the phenomenon of the self-oscillation of the economic cycles for the model of the network with different types of element couplings (cooperative and competitive). As the element of the production network there are considered the typical system of automatic control of the added value, which determines the profitability of production. *Methods.* The research methods of the theory of nonlinear dynamic systems. *Results.* Modeling of nonlinear dynamics of small ensembles of connected production elements indicates the significant role of connections, in particular, the antagonistic (competitive) relationships lead to the emergence of regular and irregular economic fluctuations (cycles).

Keywords: business cycles, nonlinear dynamics of networks, competitive couplings.

Acknowledgements. This work was supported by the Ministry of Science and Higher Education of the Russian Federation (project FSWR-2023-0031). The authors are grateful M. I. Rabinovich for useful discussions and comment.

For citation: Matrosov VV, Shalfeev VD. Dynamic model of economic cycles origin. Izvestiya VUZ. Applied Nonlinear Dynamics. 2025;33(4):513–530. DOI: 10.18500/0869-6632-003167

Introduction

Modern applied nonlinear dynamics studies processes and systems with extreme complexity. These tasks affect not only technical, physical, chemical, but also biological and socio-economic applications. The problems of the dynamics of economic systems are largely related to the study of economic fluctuations — cycles and primarily with their origin [1–4]. In this paper, we consider the model dynamics of a production network consisting of nonlinear elements - industries connected by both cooperative and antagonistic (competitive) connections. Using the example of a small ensemble of connected production elements, the influence of the nature of the connections on the possibility of fluctuations in the total output of the network, that is, on the occurrence of economic fluctuations, is studied.

The work is organized as follows. The 1 section provides brief information about economic

cycles. In the 2 section, a model of a separate production facility as an element of a production network is proposed. Sections 3, 4 present the results of numerical experiments to study the dynamics of ensembles of two and three connected productions. In last section, the conclusions are given.

1. Economic cycles

An analysis of the economic development of different countries by different economists (J. Keynes, P. Samuelson, M. Friedman, and others) led to the conclusion that the market economy is characterized by instability and irregular fluctuations in production volumes, inflation, and employment. It has been established that an economic upswing is always followed by a decrease in economic activity, which indicates the cyclical nature of a market economy. Irregular fluctuations — recurring ups and downs in the economy [5], occurring near a certain long-term trend, characterize the basic phenomenon of a market economy — economic cycles (business cycles). There are usually four phases (stages) of the economic cycle: rise (expansion), peak (boom), recession (contraction, crisis), bottom (depression, stagnation). To determine these phases, various economic indicators are used, such as GDP (gross domestic product), employment level, profit volume of enterprises, etc., as well as their combined (composite) indicator - the business cycle index [6].

To date, there are many theories that study the causes of economic cycles. These theories are based on both endogenous (internal) and exogenous (external) factors, which include natural disasters, social upheavals, technological innovations, etc. However, it should be recognized that there is no convincing general theory of economic cycles today, nor is there a single point of view on the causes of these cycles [7, 8]. It should be noted that the volume of actual GDP is the most important economic indicator that determines the economic cycle, and some authors, in particular [9], allow direct identification of fluctuations in the level of economic activity with changes in the volume of actual GDP [8]. Several methods are used to calculate GDP, in particular the value added method (production method). Value added is the difference between the cost of a product (service) produced and the cost of materials spent on its production, that is, it is a part of the cost of products added directly by the enterprise itself. Summing up the added values for all industries at the country level allows us to obtain the value of GDP for the time interval under consideration.

Thus, the task of studying the causes of economic fluctuations (business cycles), in principle, can be reduced to the study of a certain dynamic model of a production network of interconnected dynamic elements - productions, allowing an assessment of the total value added across the network (i.e., GDP) and an analysis of the dynamics of GDP changes over time depending on various network parameters and connections of elements in the network, which may eventually allow us to study the conditions for the emergence of business cycles using such a model. Let's move on to building such a model.

2. Production model

We will consider the production network model as a model of interconnected dynamic elements - productions. For each production, as an element of the network, we will consider a simple model characterized by only one variable that determines the profitability of production,

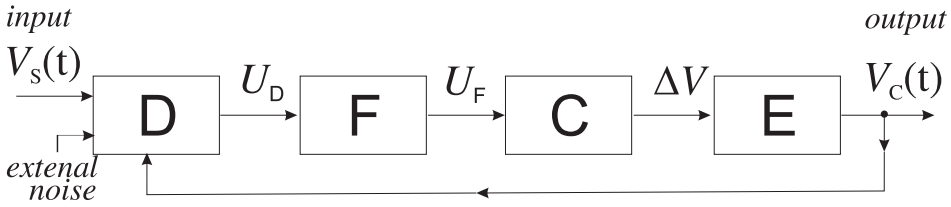

Fig. 1. Production model as a system of automatic regulation

namely the added value. As a basic model of such production, we will consider a typical automatic control system. The approach to describing the dynamic behavior of various technical, biological, social and other objects as automatic control systems is not new, and many examples of using this approach can be found in the literature, in particular [10, 11].

The model of production functioning as an automatic control system is shown in Fig. 1. Let us describe the dynamics of this system in the same way as it is done in [10]. Here E is a management object, an Estimator, which generates an estimate of the current size of the value added $V_C(t)$ at the output. The system input receives a signal $V_S(t)$ — a preset planned size of the value added. Further, for simplification, we will consider $V_S(t)$ to be a constant value over the time intervals under consideration, and the external noise is absent. The discriminator D compares the signals $V_C(t)$ and $V_S(t)$, the signal U_D from the output D passes through the filter F, which eliminates high-frequency (small-scale) fluctuations. The signal U_F from the output of the filter F enters the controller C, which acts on the active element E, changing the estimated value of $V_C(t)$ towards convergence with $V_S(t)$.

An equation describing the dynamics of an automatic control system can be obtained by writing equations for each element of the system. The output signal of the estimator E can be written as

$$V_C = V_C^0 + \Delta V, \tag{1}$$

where V_C^0 is an estimate of the value added at the initial moment of time with an open control circuit, ΔV is a change in the value of the estimate under the action of the controller C.

Assuming the linearity and inertialess of the controller C, its equation can be written as

$$\Delta V = -SU_F, \tag{2}$$

where S is the slope of the controller's characteristic, and the minus sign means that the current value of V_C is shifted by the controller towards V_S.

The equation for the filter F is written using the transfer function $K(p)$:

$$U_F = K(p)U_D. \tag{3}$$

The equation for the discriminator D is

$$U_D = E\Phi(V_C - V_S), \tag{4}$$

where E is some reference value of the discriminator output, $\Phi(V_C - V_S)$ is nonlinearity of the discriminator.

Let us introduce the following notations: the current difference between the estimated and planned size of value of added value $V = V_C - V_S$, the parameter $\sigma = SE$ is the reference correction of the output size of added value due to the action of the control circuit, the dimensionless

difference between the estimated and planned size of added value $x = V/\sigma$, the dimensionless initial difference $\gamma = (V_C^0 - V_S)/\sigma$. Taking into account the introduced notations from (1)–(4) we obtain a dynamic production model in operator form

$$x + K(p)\Phi(x) = \gamma, \qquad p \equiv d/dt. \tag{5}$$

Let us take into account the inertia of the control circuit of the model (5) in the form $K(p) = (1 + ap)^{-1}$ and, introducing the dimensionless time $\tau = t/a$, we obtain from (5) under the assumption of constancy γ the equation

$$\frac{dx}{d\tau} + x + \Phi(x) = \gamma. \tag{6}$$

It is logical to represent the nonlinearity of the discriminator as a one-parameter function with saturation

$$\Phi(x) = bx/(1 + |bx|) \tag{7}$$

or with a descending section

$$\Phi(x) = 2bx/(1 + b^2x^2). \tag{8}$$

The presence of a saturation region in the discriminator's characteristic seems a completely natural assumption. As for the presence of a descending region in the discriminator's characteristic, such a region can be interpreted as a certain unrealistic nature of the large control signals from the discriminator's output and the associated mistrust of them.

Further in the numerical experiments we will take in (8) the parameter $b \leqslant 4$. The dynamics of the model (6) under the assumptions made is determined by [12] the only stable equilibrium state $O(x^*)$, the coordinate of which $x = x^*$ is found from the equation

$$\Phi(x) = \gamma - x. \tag{9}$$

Note that the coordinate $x = x^*$ in the case of nonlinearity (8) can be located either on the ascending or descending region of the nonlinearity $\Phi(x)$; this does not affect the stability of the equilibrium state. For $x^* > 0$, production is considered profitable; for $x^* < 0$, it is considered unprofitable.

The following remark is appropriate here. In the operator model (5), by introducing various $K(p)$, one can take into account the inertia and delays of actual production. In this case, the system of differential equations corresponding to the model (5) can be of high order and allow for the presence of self-oscillatory modes, resulting in regular or chaotic fluctuations in the output variable — added value $x(\tau)$. Inertia and delays in production control can be caused, in particular, by technological features or management defects in a given production facility. A study of the production dynamics characteristics caused by inertia in control circuits is beyond the scope of this paper. Here, the emphasis is placed on studying the influence of links between production facilities on the network dynamics. Taking this circumstance into account, we will further consider the dynamics of small ensembles of two or three interconnected production units. To describe individual production units, we will use a model (6) in the form of a first-order differential equation with extremely simple dynamics—a single stable equilibrium state. Models of ensembles of two or three interconnected production units are represented by nonlinear dynamic systems defined in two- and three-dimensional phase spaces. The dynamics of these models are studied by analyzing singular trajectories (equilibrium states, separatrices, limit cycles) and their bifurcations using the DNS software suite [13].

3. An ensemble of two connected productions

Let us consider the interaction of two productions. We will focus further analysis on studying the influence of connections on the dynamics of interacting systems. Based on this, we will make simplifications: we will assume that for both systems the planned values $V_{S1} = V_{S2} = V_S$ are the same, the discriminator nonlinearities are identical, the control circuit inertias $K_1(p) = K_2(p) = K(p) = (1 + ap)^{-1}$ are the same, the parameter $\sigma_1 = \sigma_2 = \sigma$. Then the dynamics of two connected (by exchanging control signals) systems will be described by the equations

$$\begin{aligned} \frac{dx_1}{d\tau} + x_1 + \Phi(x_1) &= \gamma_1 + \delta_{21}\Phi(x_2), \\ \frac{dx_2}{d\tau} + x_2 + \Phi(x_2) &= \gamma_2 + \delta_{12}\Phi(x_1). \end{aligned} \tag{10}$$

Here δ_{21} is the coefficient of the connection from the second system to the first, δ_{12} is the coefficient of the connection from the first system to the second. We will further consider cooperative and competitive (antagonistic) connections. As an example, let us take two unidirectionally connected productions P1 and P2, let P2 affect P1. We assume that both productions are profitable, that is, the values $x_1^* > 0$ and $x_2^* > 0$. If the effect of profitable P2 on P1 leads to an increase in the profitability of P1, then such a connection can logically be called cooperative. If the effect of profitable P2 on P1 leads to a decrease in the profitability of P1 or its transition to an unprofitable one, then such a connection is called competitive (antagonistic). Thus, in the case of profitable production, with positive signs of the coefficients of the connections δ_{12}, δ_{21}, the interaction between the systems is cooperative in nature; with negative δ_{12}, δ_{21}, the interaction is antagonistic. The connection will be called strong if the modulus of the connection parameter is greater than one, weak otherwise.

The coordinates x_1^* and x_2^* of the stable equilibrium state determine the added value sizes of the first and second productions, respectively, and the sum $S = x_1^* + x_2^*$ reflects the equilibrium total gross product of two linked productions. In an ensemble of connected productions, the sizes of added values and the total gross product are determined by both the states of the interacting productions and the parameters of the connections. The influence of a neighboring system on the size of added value x_1^* depends on the state x_2^* of the neighboring system. If the value $x_2^* > 0$,

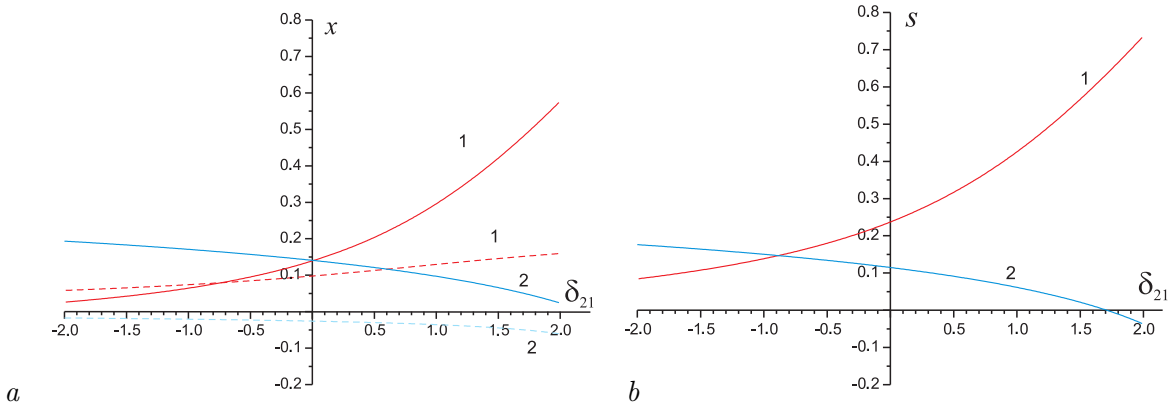

Fig. 2. Dependences of added values x_1^* (solid lines), x_2^* (dashed lines) (a) and the value of the equilibrium aggregate gross product $S = x_1^* + x_2^*$ (b) on the link parameter k_{21} for nonlinearity (7) with $\gamma_1 = 0.5, \gamma_2 = 0.2, \delta_{12} = 0.5$ — lines 1; $\gamma_1 = 0.5, \gamma_2 = -0.3, \delta_{12} = 0.5$ — lines 2 (color online)

then the cooperative connection improves the achieved value of added value, but if $x_2^* < 0$, then it worsens. In the case of an antagonistic connection, the situation is reversed. Here, a positive effect is observed when $x_2^* < 0$ and a negative one when $x_2^* > 0$. Fig. 2 illustrates the situations described above: lines 1 correspond to the case when $x_1^* > 0$, $x_2^* > 0$, lines 2 — $x_1^* > 0$, $x_2^* < 0$.

The system (10) is invariant under the substitutions $\Lambda_1 : (\gamma_1, \gamma_2, \delta_{21}, \delta_{12}, x_1, x_2) \Rightarrow (-\gamma_1, -\gamma_2, \delta_{21}, \delta_{12}, -x_1, -x_2)$, $\Lambda_2 : (\gamma_1, \gamma_2, \delta_{21}, \delta_{12}, x_1, x_2) \Rightarrow (-\gamma_1, \gamma_2, -\delta_{21}, -\delta_{12}, -x_1, x_2)$, $\Lambda_3 : (\gamma_1, \gamma_2, \delta_{21}, \delta_{12}, x_1, x_2) \Rightarrow (\gamma_1, -\gamma_2, -\delta_{21}, -\delta_{12}, x_1, -x_2)$, therefore it is sufficient to consider the dynamics of the ensemble when both connections are cooperative and when one connection is antagonistic and the other is cooperative, for example, $\delta_{21} < 0, \delta_{12} > 0$.

3.1. Dynamics of a two-production model with saturation nonlinearity. The study of the equilibrium states of the model (10) can be carried out by analyzing the principal isoclines with subsequent calculation of the Poincaré index at the points of their intersection to determine the type of singular point. As a result, it was established that for strong cooperative couplings at zero values of $\gamma_1 = 0, \gamma_2 = 0$ and $1 < b \leqslant 4$, the model (10) has three equilibrium states, two of which are stable, and one saddle. An idea of the sizes and locations of the regions of existence of the three equilibrium states of the model (10) in the parameter space is given by Fig. 3. In it, the regions of existence of the three equilibrium states are marked in gray of varying intensity depending on the values of fixed parameters of the model. From the presented pictures it follows that the bistable behavior regime in the model (10) is realized with cooperative couplings, when at least one coupling is strong. The region of existence of the bistable regime is located in the area of small values of γ. In the case of competitive connections $\delta_{21} \cdot \delta_{12} < 0$ in the phase space of the model (10) there is one stable equilibrium state; in numerical experiments, no bistable behavior regimes were identified.

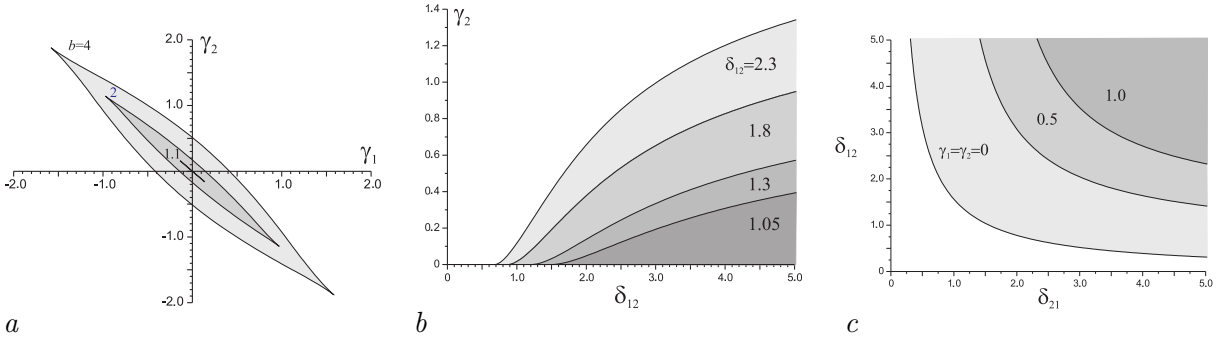

Fig. 3. Regions of existence of three equilibrium states of model (10) with nonlinearity (7) when $\delta_{21} = 1.7$, $\delta_{12} = 2.3,\ b = 4.0,\ 2.0,\ 1.1$ (a); $\gamma_1 = 0,\ b = 4.0,\ \delta_{12} = 2.3,\ 1.8,\ 1.3,\ 1.05$ (b); $\gamma_1 = \gamma_2 = 0,\ 0.5,\ 1.0,\ b = 4.0$ (c)

3.2. Dynamics of a two-production model with nonlinearity (8). A distinctive feature of nonlinearity (8) is the presence of a descending section, which leads to the existence of three equilibrium states in the model (5) for $b > 4$.

We considered the boundary value $b = 4$, when the system (5) has only one equilibrium state. Although the original model (5) with nonlinearity (8) contains only one stable equilibrium state, combining two such models into an ensemble yields a system with rich dynamics. In particular, an analysis of the behavior of the principal isoclines shows that model (10) can have up to seven equilibrium states in phase space. In Fig. 4 shows the structures of the parameter plane (γ_1, γ_2) of the model (10) for cooperative connections, when both links are strong (Fig. 4,

a), one connection is strong and the other weak (Fig. 4, b) and when both connections are weak (Fig. 4, c). Here, regions with different numbers of equilibrium states are highlighted; the total number of equilibrium states is characterized by a number enclosed in a circle. Moreover, the number of stable equilibrium states increases as the total number of equilibrium states increases and is equal to 1, 2, 3 and 4 for regions with 1, 3, 5 and 7 equilibrium states, respectively. From the presented diagrams it follows that for strong cooperative connections, the ensemble demonstrates high multistability in the region of small initial deviations γ of the estimated sizes of added value from the planned ones. A decrease in the strength of the couplings reduces the degree of multistability in the region of small γ, even to the point of complete disappearance. At the same time, at large deviations of γ, zones of bistable behavior are preserved.

Possible phase portraits of the model (10) with nonlinearity (8) are shown in Fig. 5. Let us pay attention to Fig. 5, b and Fig. 5, c, where phase portraits from the parameter domain with five equilibria and close parameter values are presented. Here, despite the proximity of the parameters, the basins of attraction of the equilibrium states 5 and 7 differ significantly. In Fig. 5, b the stationary regime determined by the equilibrium state 5 cannot be realized under the initial conditions from the fourth quadrant of the phase plane, and in Fig. 5, c the stationary regime determined by the equilibrium state 7 cannot be realized under the initial conditions from the second quadrant. The redistribution of phase flows to the equilibrium states 5 and 7 occurs as a result of the coincidence of the outgoing separatrix s of saddle 4 and the incoming separatrix

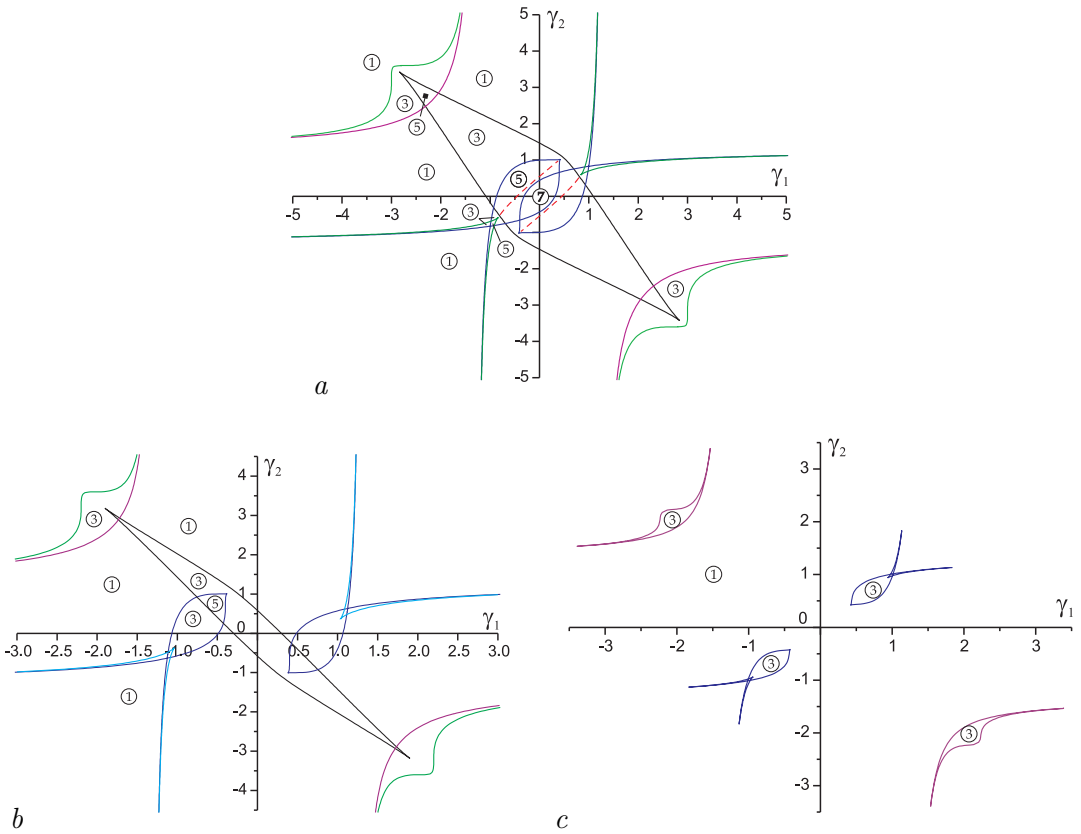

Fig. 4. Partitioning the plane (γ_1, γ_2) of parameters of model (10) with nonlinearity (8) into regions with different numbers of equilibrium states when $b = 4.0$, $\delta_{21} = 1.7, \delta_{12} = 2.3$ (a); $\delta_{21} = 0.9$, $\delta_{12} = 2.3$ (b); $\delta_{21} = 0.9$, $\delta_{12} = 0.9$ (c) (color online)

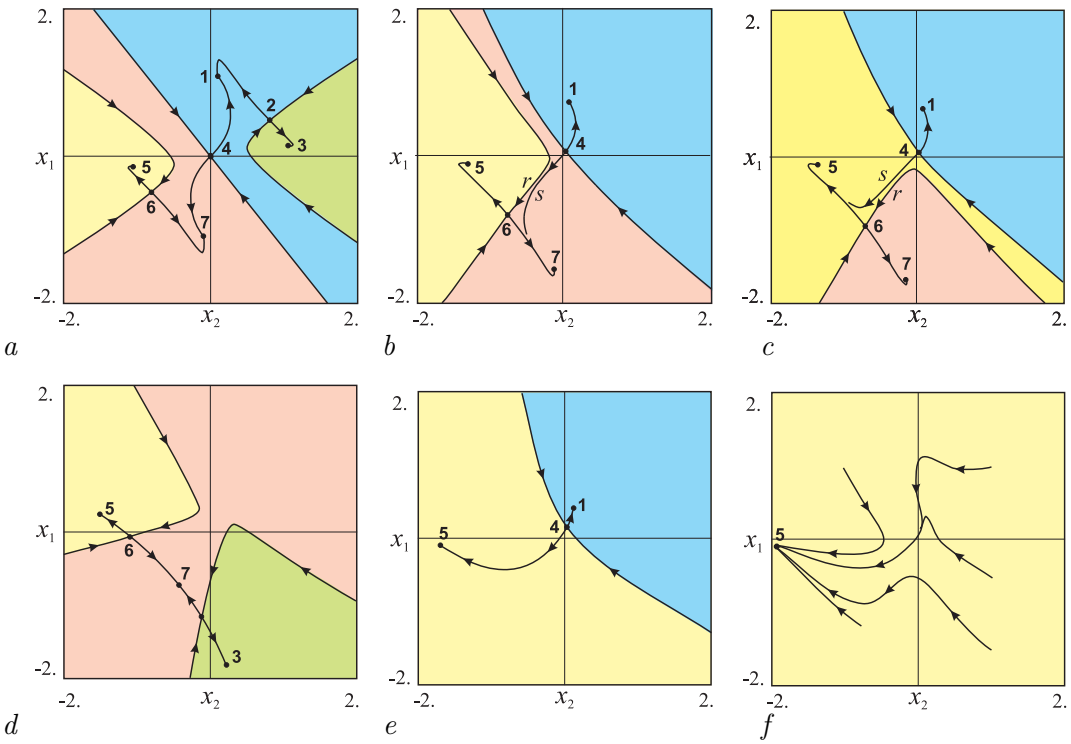

Fig. 5. Phase portraits of the model (10) with nonlinearity (8) at δ_{21}=1.7, δ_{12}=2.3, b=4 γ_1=γ_2=0 (a); γ_1= −0.4, γ_2=0 (b); γ_1= −0.5, γ_2=0 (c); γ_1= −0.9, γ_2= −0.7 (d); γ_1= −0.95, γ_2=0 (e); γ_1= −1.1, γ_2=0 (f) (color online)

r of saddle 6. The bifurcation curves responsible for the formation of heteroclinic trajectories are drawn by dashed lines in Fig. 4, *a*.

An idea of the structure of the parameter plane (γ_1, γ_2) of the model (10) with nonlinearity (8) under competitive connections is given by Fig. 6. It shows pictures when both connections are strong (Fig. 6, *a*), one connection is strong, the other weak (Fig. 6, *b*) and when both connections are weak (Fig. 6, *c*).

The figures show that parameter regions with multistable ensemble behavior exist in the presence of at least one strong coupling, and they are located in the region of large γ. In the case of weak couplings, an ensemble of two coupled industries can exhibit bistable behavior, which is also observed at large γ. Multistable behavior of the system (10) leads to hysteresis phenomena.

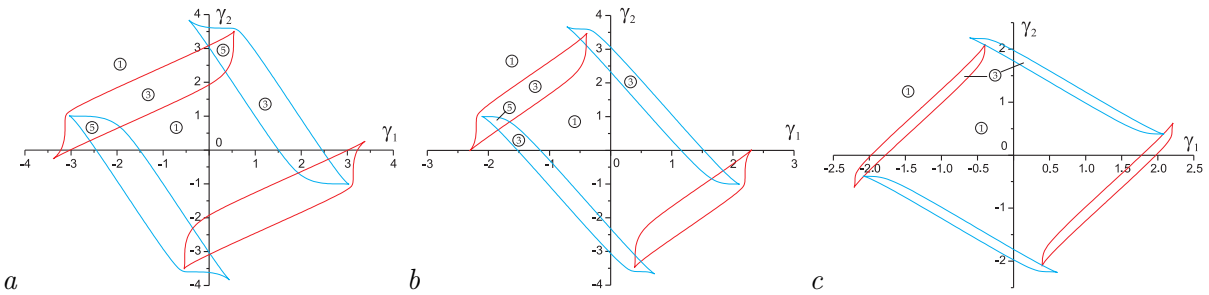

Fig. 6. Partitioning the plane (γ_1, γ_2) of parameters of model (10) with nonlinearity (8) into regions with different numbers of equilibrium states when $b = 4.0$, $\delta_{21} = -1.83$, $\delta_{12} = 2.3$ (a); $\delta_{21} = -0.9$, $\delta_{12} = 2.3$ (b); $\delta_{21} = -0.9$, $\delta_{12} = 0.9$ (c) (color online)

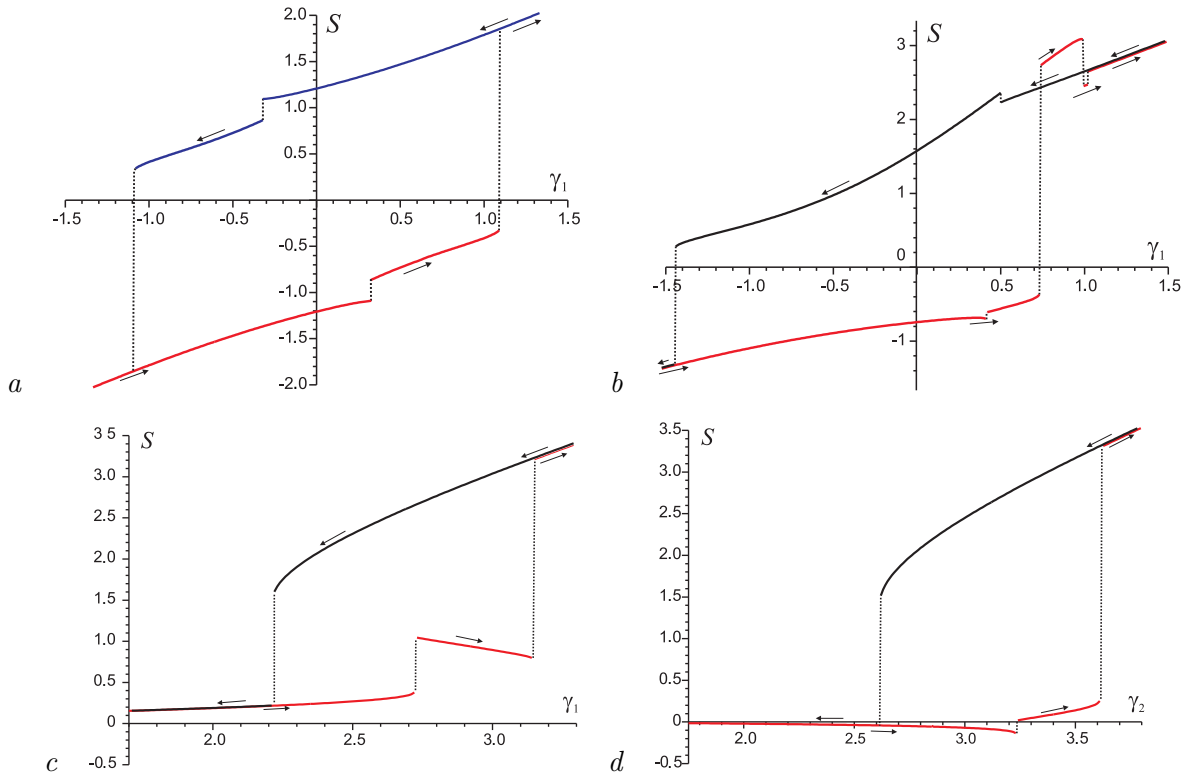

Fig. 7. Examples of dependencies of the value of the equilibrium aggregate gross product S, calculated using the model (10) with nonlinearity (8) at $b = 4$, $\delta_{21} = 1.7, \delta_{12} = 2.3$, $\gamma_2 = 0$ (a) и $\gamma_2 = 0.7$ (b); $\delta_{21} = -1.83, \delta_{12} = 2.3$, $\gamma_2 = -0.5$ (c) and $\gamma_1 = 0.2$ (d) (color online)

Examples of ambiguous behavior of the model of two coupled industries are shown in Fig. 7. Here, the solid lines reflect changes in the equilibrium aggregate gross product S, dashed lines reproduce stepwise changes in the gross product, and arrows indicate the direction of parameter change.

As for self-oscillatory modes in the ensemble of two coupled industries, they were not detected during numerical experiments with the model (10).

4. An ensemble of three connected productions

Let us consider the interaction of three productions (Fig. 8). Further we will assume that for all systems the planned values $V_{S1} = V_{S2} = V_{S3} = V_S$ are the same, the discriminator nonlinearities are identical, the control circuit inertias $K_1(p) = K_2(p) = K(p) = (1 + ap)^{-1}$ are the same, the parameter $\sigma_1 = \sigma_2 = \sigma_3 = \sigma$.

Then the dynamics of the three coupled

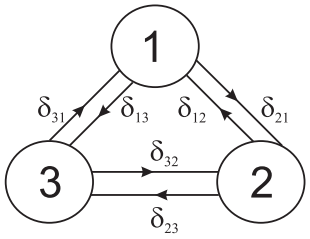

Fig. 8. Scheme of interaction of three productions

systems will be described by the equations

$$\begin{aligned}
\frac{dx_1}{d\tau} + x_1 + \Phi(x_1) &= \gamma_1 + \delta_{21}\Phi(x_2) + \delta_{31}\Phi(x_3),\\
\frac{dx_2}{d\tau} + x_2 + \Phi(x_2) &= \gamma_2 + \delta_{12}\Phi(x_1) + \delta_{32}\Phi(x_3),\\
\frac{dx_3}{d\tau} + x_3 + \Phi(x_3) &= \gamma_3 + \delta_{13}\Phi(x_1) + \delta_{23}\Phi(x_2),
\end{aligned} \tag{11}$$

where δ_{ij} are the coefficients of connections from the i-th system to the j-th.

An ensemble of three elements can be viewed as a union of three intersecting pairs: $\{1,2\}, \{1,3\}, and \{2,3\}$. Each pair, depending on the parameters of the connections, has its own partition in the plane of parameters corresponding to γ.

4.1. Dynamics of a three-production model with saturation nonlinearity (7). Let us take a pair $\{1,2\}$ with nonlinearity (7) and parameters b=3.7, γ_1=0.6, γ_2=0.5, δ_{12}=2.6, $\delta_{21} = 4.6$. In this case, the structure of the phase portrait of the model (10) is determined by three equilibrium states: $O_1(x^*_{11} = 3.72,\ x^*_{21} = 2.04)$, $O_3(x^*_{13} = -2.14,\ x^*_{23} = -1.02)$ — stable nodes and $O_2(x^*_{12} = -0.12,\ x^*_{22} = -0.077)$ — saddle. We connect the pair $\{1,2\}$ by unidirectional links with the third element at $\gamma_3 = 0.54$, the dynamics of which is determined by the stable equilibrium state with coordinate $x^*_3 = 0.16$. The ensemble constructed in this way inherits the structure of the phase space of the pair $\{1,2\}$ model. In the case of cooperative connections $\delta_{13} = 0.75, \delta_{23} = 4.6$ the structure of the phase portrait of the model (11) is determined by the stable equilibrium states $O_1(x^*_{11}$=3.72, x^*_{21}=2.04, x^*_{31}=2.71), $O_3(x^*_{13}$=−2.14, x^*_{23}=−1.02, x^*_{33}=−1.42) and the saddle $O_2(x^*_{12} = -0.12,\ x^*_{22} = -0.077,\ x^*_{32} = -0.08)$. For antagonistic connections $\delta_{13} = -0.75$, $\delta_{23} = -4.6$ the model (11) also has two stable equilibrium states $O_1(x^*_{11} = 3.72, x^*_{21} = 2.04, x^*_{31} = -1.68)$, $O_3(x^*_{13} = -2.14, x^*_{23} = -1.02, x^*_{33} = 2.44)$ and a saddle $O_2(x^*_{12} = -0.12, x^*_{22} = -0.077, x^*_{32} = 0.66)$.

The influence of feedbacks from the third element to the first two is illustrated in Fig. 9. Here *line* l_1 corresponds to the merging of the equilibria O_3 and O_2; line l_2 — the emergence of two new equilibria O_4 and O_5. *Line* l_2 contains the neutrality point n_1, which divides this line into two sections. The section of the curve marked by the solid line corresponds to the merging of the stable and saddle equilibria, and the section of the curve marked by the dashed line corresponds

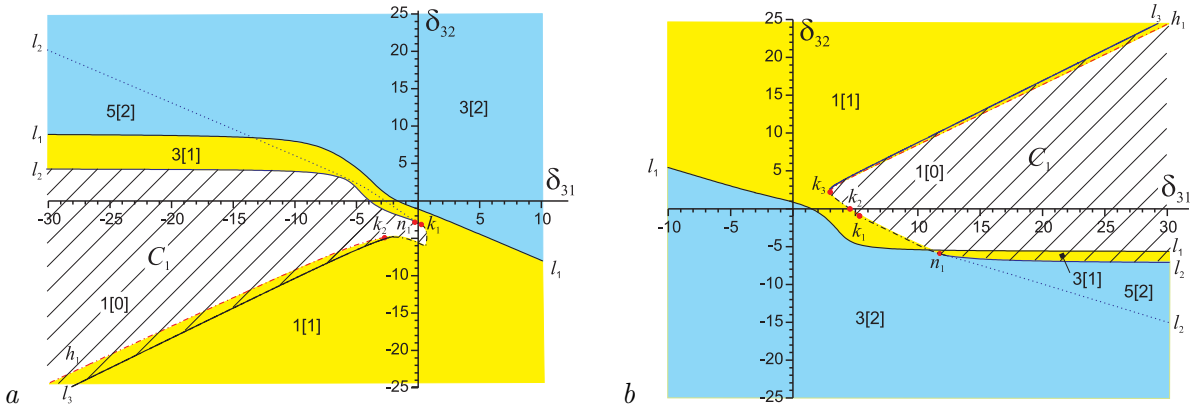

Fig. 9. Parametric portrait of the (11) when b=3.7, γ_1=0.6, γ_2=0.5, γ_3=0.54, δ_{12}=2.6, $\delta_{21} = 4.6$ at $\delta_{13} = 0.75$, $\delta_{23} = 2.7$ (a) and $\delta_{13} = -0.75$, $\delta_{23} = -2.7$ (b) (color online)

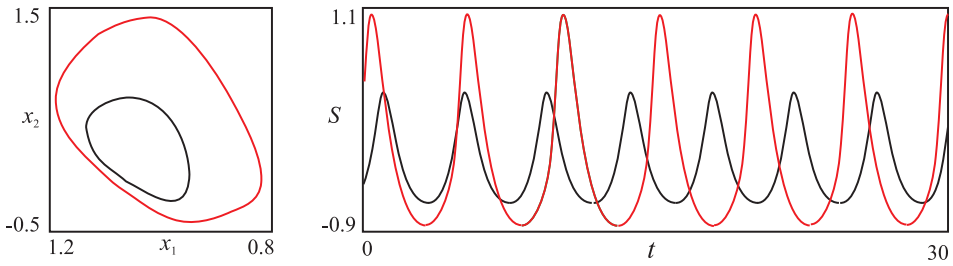

Fig. 10. Example of bistable self-oscillatory behavior of the model (11) and the corresponding dependence $S(t) = x_1 + x_2$ at b=3.7, γ_1=0.6, γ_2=0.5, γ_3=0.54, δ_{12}=2.6, $\delta_{21} = 4.6$, $\delta_{13} = -0.75$, $\delta_{23} = -2.7$, $\delta_{31} = 10$, $\delta_{32} = -4.72183$ (color online)

to the merging of unstable equilibria. Point n_1 is the endpoint for *curve* h_1 of the Andronov–Hopf bifurcation curve (dash-dotted line). At points k_i on line h_1, the first Lyapunov value vanishes. Points k_i divide the h_1 curve into regions of soft and hard oscillation excitation. The regions of the curve with hard oscillation excitation in Fig. 9 are marked in red, while those with soft oscillation excitation are marked in black. The mechanism of hard oscillation excitation is preceded by a tangential bifurcation (on line l_3), resulting in the appearance of stable and unstable limit cycles in the phase space of the model (11).

Thus, the lines $l_1 - l_3, h_1$ divide the plane of parameters $(\delta_{31}, \delta_{32})$ into regions with different numbers of equilibrium states and dynamic behavior. In Fig. 9, the selected regions are characterized by a pair of numbers, where the first number reflects the total number of equilibrium states in a given region, and the number in square brackets is the number of stable equilibrium states. Here, the regions with one stable equilibrium state are also highlighted in yellow, the regions with two stable equilibrium states are highlighted in blue, and the region C_1 of existence of self-oscillatory modes is marked by hatching. It is established that in the region C_1 two self-oscillatory modes can simultaneously exist. Fig. 10 shows the projections of simultaneously existing stable limit cycles. The region of the bistable self-oscillatory mode is small, therefore it is not marked in Fig. 9.

4.2. Dynamics of a three-production model with nonlinearity (8). Let us take a pair $\{1, 2\}$ with nonlinearity (8) and parameters γ_1=0.6, γ_2=0.5, δ_{21}=4.6, δ_{12}=2.6, b=3.7 and connect it with a unidirectional positive connection to the third element, where $\delta_{13} = 0.75$, $\delta_{23} = 2.7$. For the chosen parameter values, the phase portrait is determined by three stable equilibrium states: $O_1(3.87, 0.12, 2.4258)$, $O_3(-1.26, -0.07, -0.18)$ and $O_5(-0.16, -1.45, -0.19)$, as well as saddles $O_2(-0.038, -0.027, -0.025)$, $O_4(-0.53, -1.22, -0.23)$ with separatrices. For zero constraints $\delta_{13} = \delta_{23} = 0$, the third element of the ensemble has one stable stationary equilibrium state at the point $x_3^* = 0.68$. Next, we will analyze the influence of the feedback parameters δ_{31} and δ_{32} from the third element to the first and second elements of the ensemble.

Fig. 11 shows a map of the dynamic regimes of the model (11) on the plane $(\delta_{31}, \delta_{32})$. Here, the regions where the system (11) has a different number of stable equilibrium states (stationary regimes) are painted in different colors. In addition, each color of the region is associated with a number that reflects the number of stable equilibrium states in this region. The structure of the partition is determined by the solid lines $l_1 - l_{10}$, corresponding to the bifurcation of two-fold equilibrium states (saddle-node bifurcation), as well as the dash-dotted lines $h_1 - h_7$, reflecting the Andronov–Hopf bifurcations. The bifurcation curves $h_1 - h_7$ adjoin the curves $l_1 - l_9$ at the neutrality points n_i. The lines marked in black correspond to a soft transition from stable

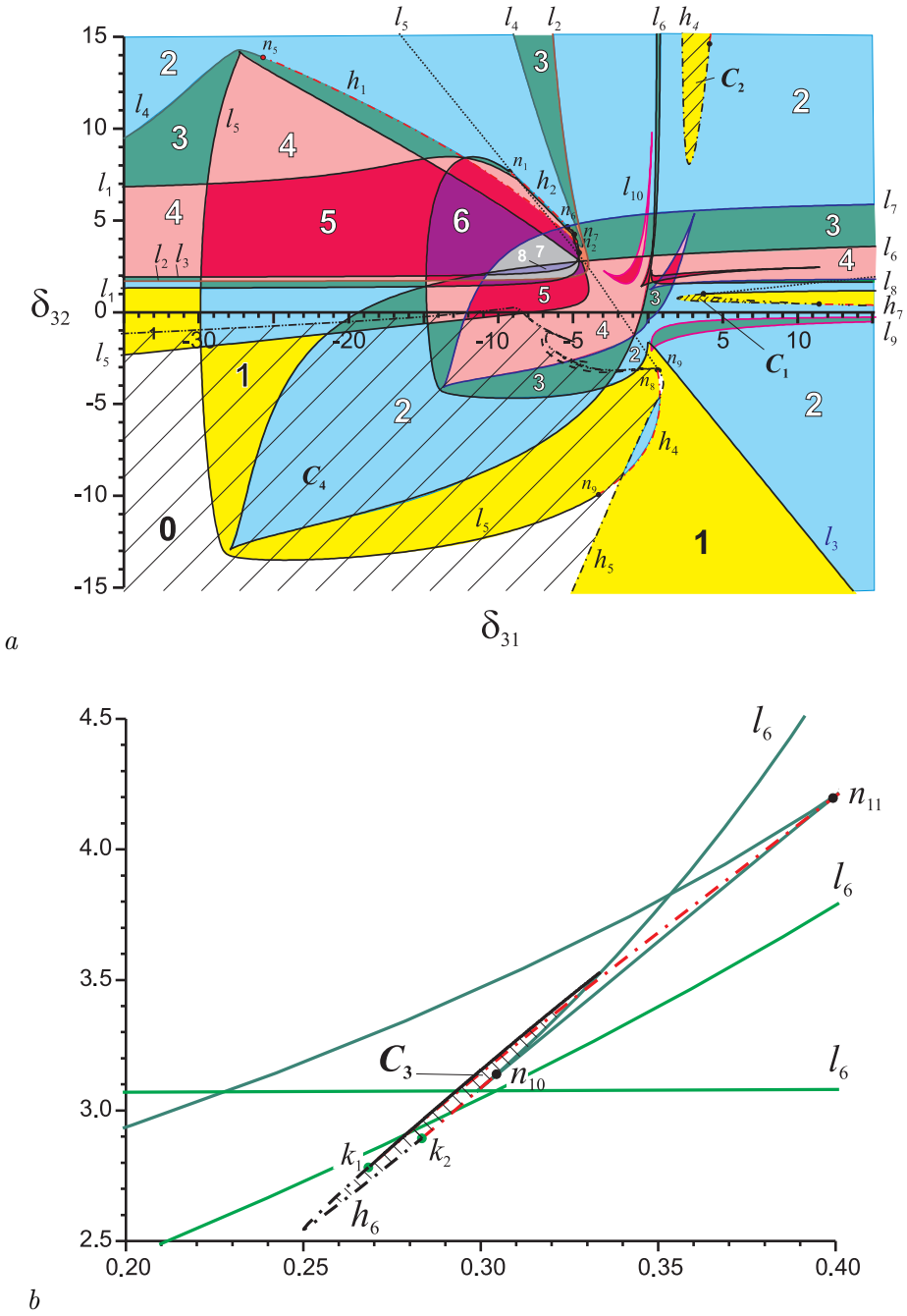

Fig. 11. Parametric portrait of the (11) when $\gamma_1 = 0.6$, $\delta_{21} = 4.6$, $\delta_{12} = 2.6$, $\gamma_2 = 0.5$, $\delta_{23} = 2.7$, $\delta_{13} = 0.75$, $\gamma_3 = 0.54$, $b = 3.7$ (a), enlarged fragment of parametric portrait (b) (color online)

equilibrium to stable limit cycles in the phase space. The red dash-dotted curve characterizes a hard transition from stable equilibrium to stable limit cycles, where stable limit cycles do not arise. The dots separating the differently colored sections correspond to the vanishing of the first Lyapunov value. The dashed lines l_5 and l_8 reflect the merging and disappearance of unstable equilibrium states. These bifurcations do not significantly affect the attractor dynamics of the model (11); lines l_5 and l_8 are included to provide a more complete understanding of the bifurcation transitions. From the analysis of the presented partition of the plane $(\delta_{31}, \delta_{32})$, taking

into account that the remaining connections are cooperative [1], it follows:

- the combination of three elements with a single stationary state through cooperative connections leads to an increase in the number of stable steady-state regimes. In the case under consideration, the number of simultaneously existing stable equilibrium states can reach six. The largest regions of multistable behavior are regions with two, three, and four stable equilibrium states;
- in an ensemble of three elements connected by cooperative connections, regular self-oscillatory modes can be realized;
- in an ensemble of three elements linked by competitive connections, the number of simultaneously existing stable stationary modes can reach eight. There are also connection parameter values where stable stationary modes are absent from the ensemble; in this case, a self-oscillatory mode is realized.

In Fig. 11, the regions of existence of self-oscillatory modes C_1–C_4 are marked with shading. Region C_1, located in the first quadrant of the parametric portrait, is bounded by the curves of the supercritical Andronov-Hopf bifurcation (dash-dotted line) and the double limit cycle (the lower boundary of region C_1). From above, region C_1 is bounded either by bifurcation lines of separatric loops of varying bypass strength or by crisis lines of the chaotic attractor. The chaotic attractor arises as a result of a cascade of period-doubling bifurcations for large values of δ_{31}.

Region C_2 is located in the first quadrant. Its boundaries are the Andronov-Hopf bifurcation curves (dash-dotted line) and the double limit cycle bifurcation curve (solid line, adjacent to the point where the first Lyapunov value vanishes). The self-oscillatory regime realized for parameter values from region C_2 is regular and does not bifurcate with parameter variations within the region.

Due to its small size, region C_3 is shown in fragment 11, *b*. Its boundaries are the Andronov-Hopf bifurcation curves, the double limit cycle (tangent bifurcation), and the saddle-node separatrices. In the fragment, the first Lyapunov value vanishes at points k_1 and k_2.

Region C_4 is the largest region. It is located in the third quadrant, that is, where the coupling parameters δ_{31} and δ_{32} are antagonistic. Note that for large values of δ_{31} and δ_{32}, the self-oscillatory regime becomes globally stable; with decreasing δ_{31} and δ_{32}, the global stability of the limit cycle is violated by stable equilibria, and the limit cycle itself can lose stability through period-doubling bifurcations, turning into a chaotic attractor (Fig. 12). In Fig. 11, the bifurcation curve characterizing the first period doubling is drawn by the dotted line. The region of existence of chaotic oscillations in the third quadrant is somewhat larger than in the first, but still small. Region C_4, where the self-oscillatory regime is globally stable, is highlighted in dark gray.

From the analysis of self-oscillatory modes it follows:

- In cooperative constraints, there are several regions in the parameter space where self-oscillatory modes are realized—regions C_1, C_2, and C_3. The regions where self-oscillatory modes exist are small, and the self-oscillatory modes themselves are not globally stable. In region C_2, the self-oscillatory mode can be either regular or chaotic.
- In the case of competitive connections, the region of existence of the self-oscillatory regime C_4 is significantly larger than the regions C_1, C_2, and C_3. The self-oscillatory regime can be either regular or chaotic, and the regular self-oscillatory regime can be globally stable.

[1] The first quadrant reflects the case when the elements of the ensemble are united only by cooperative connections — all connections are positive, in the remaining quadrants the connections are competitive.

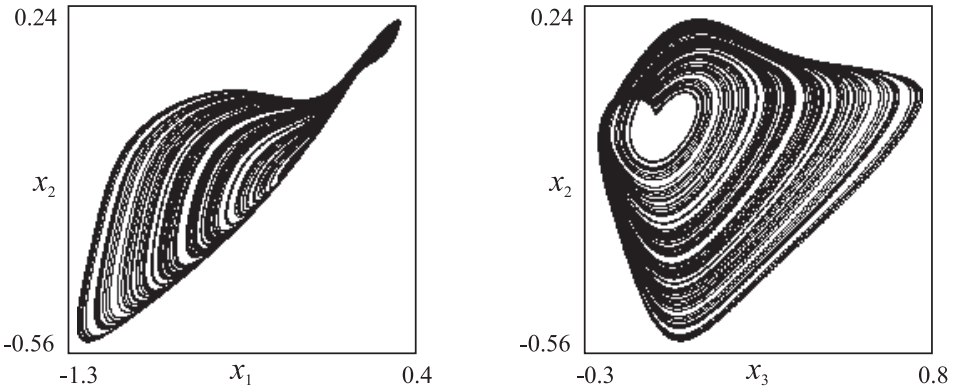

Fig. 12. Projections of chaotic attractors of (11) when $\gamma_1 = 0.6$, $\delta_{21} = 4.6$, $\delta_{12} = 2.6$, $\gamma_2 = 0.5$, $\delta_{23} = 2.7$, $\delta_{13} = 0.75$, $\gamma_3 = 0.54$, $b = 3.7$, $\delta_{31} = -4.5$, $\delta_{32} = -2.87$

Now let us consider a pair $\{1, 2\}$ with nonlinearity (8) with competitive (antagonistic) connections $\delta_{21} = -4.6$, $\delta_{12} = -2.6$, $b = 3.7$ and connect it with unidirectional negative connections to the third element, where $\delta_{13} = -0.75$, $\delta_{23} = -2.7$. For $\gamma_1 = 0.6$, $\gamma_2 = 0.5$, the phase portrait of the model (11) defines three stable equilibria: $O_1(-0.1,\ 1.84,\ 0.028)$, $O_3(1.63,\ -0.04,\ 0.18)$ and $O_5(-3.0,\ 0.14,\ -1.07)$, as well as saddles $O_2(0.02,\ 0.01,\ 0.02)$, $O_4(-1.35, 0.99, -0.18)$ with one-dimensional outgoing separatrices. The influence of feedbacks from the third element of the ensemble to the pair $\{1, 2\}$ is reflected in Fig. 13, which represents a partition of the plane of parameters δ_{31} and δ_{32} into regions with different numbers of stable equilibria, which are marked with different colors, as well as a number reflecting the number of stationary regimes. The boundaries of the selected regions are the curves of the bifurcations of the double equilibrium

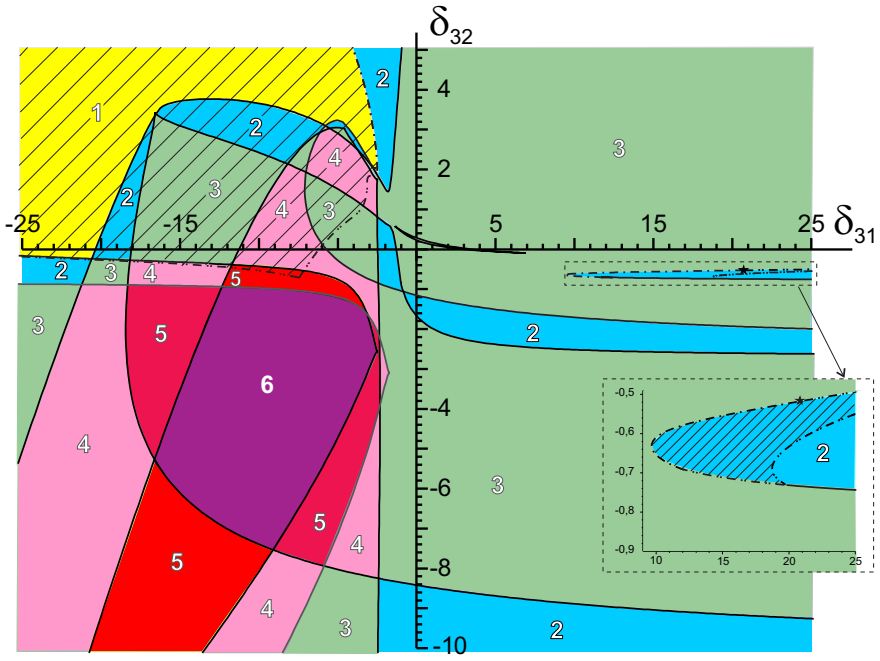

Fig. 13. Parametric portrait of the (11) when $\gamma_1 = 0.6$, $\delta_{21} = 4.6$, $\delta_{12} = -2.6$, $\gamma_2 = 0.5$, $\delta_{23} = -2.7$, $\delta_{13} = -0.75$, $\gamma_3 = 0.54$, $b = 3.7$ (color online)

state — solid lines and the Andronov–Hopf — dash-dotted lines. The shading marks the regions for which a regular self-oscillatory regime exists for the parameter values. These regions are bounded by the dash-dotted line of the soft Andronov–Hopf bifurcation, as well as by the dash-dotted line with two dots, which includes the bifurcation curves of the separatrices loop, the double limit cycle, and the period-doubling bifurcation. Note that for the considered values of the parameter, the period-doubling bifurcation is hard, which does not lead to a doubling of the periods of the self-oscillatory regimes. The existence of chaotic oscillations has not been established.

Thus, the conducted analysis allows us to conclude that the connections in ensembles of interconnected production elements are important. The collective behavior of elements in an ensemble is determined both by the number of elements in the ensemble and by the evaluation rule for the compared added value sizes (the type of nonlinearity Φ of the discriminator D). It can be concluded that increasing the number of elements in an ensemble with initially unambiguous stationary behavior leads to the emergence of zones of multistable behavior in the parameter space of model models, leading to the emergence of self-oscillatory regimes, both regular and chaotic.

Conclusion

This paper examines the dynamics of an endogenous production network model depending on the type of connections between production elements. Network elements were modeled as automatic control systems. The economic indicator, value added, was adopted as the controlled variable, allowing us to study the model dynamics of gross value added across the entire network and, consequently, the dynamics of GDP change. Numerical experiments with small ensembles of elements demonstrated that the inclusion of cooperative and competitive connections between network elements leads to the emergence of regular and chaotic fluctuations in GDP dynamics, that is, to the emergence of economic cycles. Naturally, our proposed model cannot be used as a basis for forecasting specific data on real economic cycles; however, it allows us to conclude that the proposed model and approach are promising for further experiments studying the qualitative characteristics of economic fluctuations, their causes, and the nature of their dependence on economic connections between market participants.

References

1. Kuznetsov YA. Mathematical modeling of economic cycles: facts, concepts, results. Economic Analysis: Theory and Practice. 2011;10(17):50–61 (in Russian).
2. Kuznetsov YA. Mathematical modeling of economic cycles: facts, concepts, results (end). Economic Analysis: Theory and Practice. 2011;10(18):42–56 (in Russian).
3. Matrosov VV, Shalfeev VD. Simulation of business and financial cycles: Self-oscillation and synchronization. Izvestiya VUZ. Applied Nonlinear Dynamics. 2021;29(4):515–537 (in Russian). DOI: 10.18500/0869-6632-2021-29-4-515-537.
4. Matrosov VV, Shalfeev VD. Simulation of the business-cycle synchronization processes in an ensemble of coupled economic oscillators. Radiophys. Quantum Electron. 2022;64(10): 750-759. DOI: 10.1007/s11141-022-10176-1.
5. Samuelson P., Nordhaus W. Economics. New York: McGraw Hill; 1992. 784 p.
6. Baxter M, King RG. Measuring business cycles: approximate band-pass filter for economic time series. The Review of Economics and Statistics. 1999;81(4):575–593. DOI: 10.1162/003

465399558454.
7. Hansen AH. Business Cycles and National Income. New York: Norton, 1951. 639 p.
8. Lebedeva AS. The genesis of economic cycle theory. Int. Research Journal. 2013;(8):31–34.
9. Vechkanov GS, Vechkanova GR. Macroeconomics. M.: Piter; 2002. 240 p.
10. McCullen NJ, Ivanchenko MV, Shalfeev VD, Gale WF. A dynamical model of decision-making behaviour in network of consumers withb application to energy choices. Int. J. Bifurc. Chaos. 2011;21(9):2467–2480. DOI: 10.1142/S02.18127411030076.
11. Shalfeev V, Matrosov VV. Nonlinear Dynamics of Phase Synchronization Systems. Nizhny Novgorod: Nizhny Novgorod University Publishing; 2013. 366 p. (in Russian).
12. Andronov AA, Vitt AA, Khaikin SE. Theory of Oscillators. New York: Dover Publ.; 1987. 815 p.
13. Matrosov VV. Dynamics of Nonlinear Systems: Software Complex for Studying Nonlinear Dynamical Systems with Continuous Time. Nizhny Novgorod: Nizhny Novgorod University Publishing; 2002. 54 p. (in Russian).